

Kenneth R. Knapp\* and John Bates  
NOAA - National Climatic Data Center, Asheville, North Carolina

## 1. INTRODUCTION: ISCCP

The International Satellite Cloud Climatology Project (ISCCP) has provided data for numerous studies of the Earth's climate. ISCCP cloud and radiance information are derived from geostationary and polar-orbiting satellites for the time period of 1983 through the present. However, one ISCCP data set – level B1 – has seen little research despite its 20 year record at the National Climatic Data Center (NCDC). At first this was due to the volume of the B1 data, in the context of computing capabilities of the 1980's. But by the time computing power caught up with the B1 volume, data had already languished for years with little documentation, and no support software or quality control. Thus, in light of the capability to process the entire B1 data set (merely 1.2 Tb at present) for climate research, it becomes necessary to assess and correct these deficiencies.

There are many benefits in using the B1 data, since they have:

- near global coverage,
- 3-hour temporal sampling,
- approximately 10 km spatial sampling, and
- the only GMS data from 1983-1987 (at such a high resolution).

Thus, work at NCDC is ongoing to compile B1 data documentation, develop input and output software, test data quality and make them accessible.

The following describes how the B1 data set relates to the ISCCP dataflow, the details of the B1 coverage and a few examples of climate applications possible with this new data set.

## 2. ISCCP DATAFLOW

To better understand the B1 data set, one must first understand the ISCCP data processing.

### 2.1 ISCCP Data Processing

The ISCCP Satellite Processing Centers (SPCs) are the primary data providers. The SPCs provide subsampled data (level B) to the GPC as

well as the ISCCP Central Archive (ICA). Level B1 is the first level of sub-sampling (detailed below) and is only sent to the ICA. The second level of sub-sampling is the B2, (which has roughly one-third the spatial resolution of the B1 data) which is sent to the Global Processing Center (GPC).

The GPC quality controls the B2 data and creates the B3 data set, which merges the data into one format. Cloud and radiation products (level D data) are then derived from the B3 data, providing the most complete cloud data set (at 3-hourly resolution for 20 years) to date.

### 2.3 B1 Data: A hodgepodge of data formats

So, ISCCP B1 data are sent to ICA and stored, but never officially used. Aside from migrating the data stores to new media, the B1 data have largely been untouched since the original ingest. The entire data set consists of more than 240,000 files which originate from 5 different SPCs and 18 satellites. The data from the various SPCs are in a variety of formats with varying levels of documentation from fully documented (each bit defined) to none whatsoever.

Since beginning this work, a mostly complete set of documentation has been compiled by bringing together various resources and data descriptions. Those data sets initially without format descriptions have been investigated, and some were found to be similar to other data formats. Scientists at CIRA, Japan Meteorological Agency (in particular for translating documents to *English*) and GPC proved invaluable.

## 3. B1 DATA COVERAGE

### 3.1 Spectral Coverage

The primary channels for ISCCP cloud analysis are the visible channel (a broad channel centered near 0.6  $\mu\text{m}$ ) and an infrared channel in the IR window region (near 11  $\mu\text{m}$ ) which have been on every meteorological geostationary satellite since 1983. The relative similarity of the channels has allowed cross-calibration and has been used to estimate cloud properties including optical depth and cloud top.

Information at other channels are also available from the ISCCP B1 data. In particular, the Meteosat-series of satellites has provided

---

\* Corresponding author address: Kenneth Knapp; NCDC/RSAD; 151 Patton Ave.; Asheville, NC, 28801; email: Ken.Knapp@noaa.gov

water vapor imagery (near 6.7  $\mu\text{m}$ ) since its inception. Also, the newer GOES-series (beginning with GOES-8) provide similar water vapor imagery along with near IR ( $\sim 3.9 \mu\text{m}$ ) and IR split-window ( $\sim 12 \mu\text{m}$ ) channels. Thus, the ISCCP IR/visible cloud detection tests can be compared with the spectral tests now possible. And in the future, new satellite sensors will provide more spectral channels (such as Meteosat Second Generation), allowing for more thorough cloud retrievals.

### 3.2 Spatial Coverage

The spatial coverage of the B1 data set includes most of the world. The primary deficiency is lack of observations of the poles (which is made up for in ISCCP data by incorporating AVHRR observations). Otherwise, coverage is continuous when satellite data are available. Times when data are unavailable include random missing observations (i.e., files never delivered by the SPC) and systematic gaps in the data coverage. In particular, the lack of geostationary observations over the Indian Ocean is prominent. Until recently, these data were not made available, so a gap exists in the merged imagery. This was overcome when EUMETSAT moved the Meteosat-5 to 63° East in 1997 to support the Indian Ocean Experiment (INDOEX), where it remains to present.

The spatial resolution of the B1 data is roughly 8 km at the Equator. Sub-sampling for most of the sensors constituted taking every other observation in the IR which generally had 4 km resolution. The exception to this is the Meteosat series which had an IR resolution of 5 km, so the B1 resolution is 10 km. Also, the visible channels tend to have finer

resolutions than their IR counterpart. In such cases, the visible pixels were averaged to the IR resolution (4 or 5 km, depending on the sensor), then subsampled to the B1 resolution.

### 3.3 Temporal Coverage

The temporal span of ISCCP B1 data is July 1983 to present. During this time, more than 18 satellites have contributed to the data record, see Figure 1. Observations are made from each satellite full disk observation nearest the synoptic time (00, 03, 06, ..., 21 UTC), IR imagery is provided each time period while visible imagery is generally dropped for times near the satellite local midnight.

## 4. B1 CLIMATE APPLICATIONS

Climate applications that would benefit from B1 data abound. For example, once the data set undergoes some basic preprocessing, the data set could be used to extend the current data coverage for the Global Precipitation Climatology Project (GPCP). Other applications are possible, some of which are described below.

### 4.1 Preprocessing

Data preprocessing, that is, the necessary means to perform science with the B1 data includes 3 steps: navigation, quality control, and calibration.

Image navigation is crucial to satellite applications because it provides the geolocation of image pixels, determining such things as land or water pixel classification and viewing/illumination geometry. Initially the satellites were spin-stabilized, but the newer GOES-8 series is 3-axis

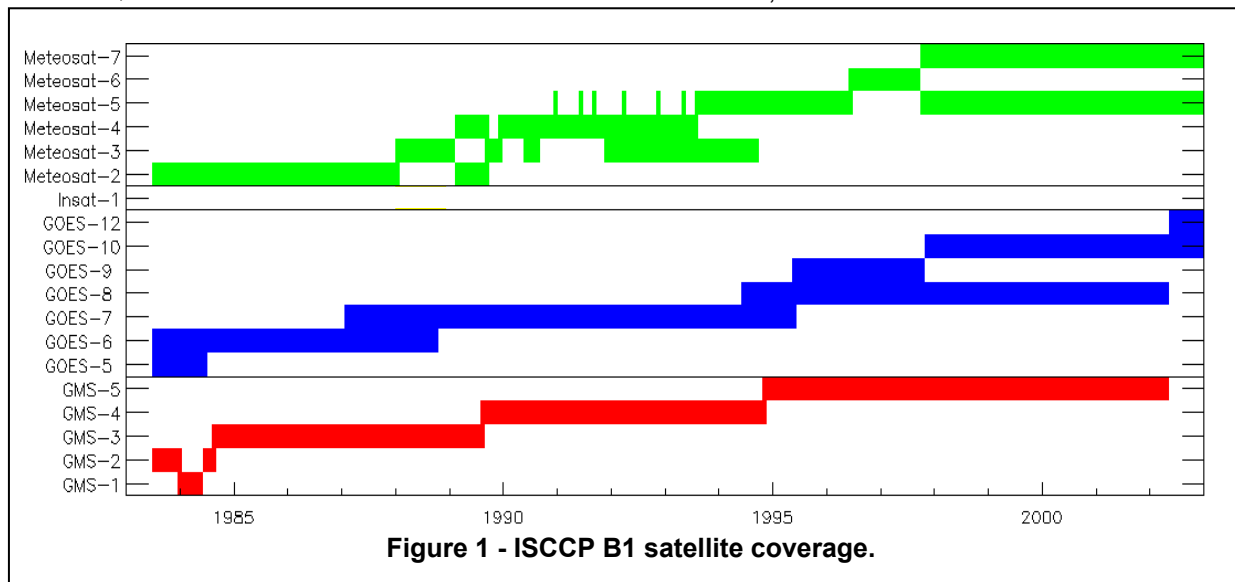


Figure 1 - ISCCP B1 satellite coverage.

stabilized, each providing different navigation algorithms. Among the spin-stabilized satellites, a variety of navigation styles were employed. Among them were: Keplerian orbital elements, Chebyshev polynomials of the orbit, satellite position and velocity components, and rectification of the satellite image to a fixed view (as done for Meteosat). Navigation accuracy can be tested through comparisons with coincident imagery from other geostationary and polar satellites.

The B1 data are provided with little information on data quality. Current work is on-going to assess the data quality using basic statistics of the on-earth and off-earth pixels. For instance, the averages of the on-earth IR pixels for the Meteosat-5 record are shown in Figure 2. The trend for the more than 6 years of data is rather uniform, except for: discontinuities (which are likely changes in the calibration) and outliers. Calibration adjustments should remove discontinuities, but the significant outliers are likely bad data and should be removed from analysis.

Calibration is perhaps the simplest of the B1 preprocessing steps. ISCCP processing includes a thorough cross-calibration between geostationary sensors as well as with AVHRR (performed by the ISCCP Satellite Calibration Center). The B1 count values are identical in nature to those in the B3 data set; only the spatial resolution is different. Thus the ISCCP B3 calibration can be used to calibrate B1 data. Tests will be made to check for long-term stability of sensors, but these are likely to show minimal trends given the ISCCP calibration. For instance, Rigollier et al. (2002) calibrate Meteosat data using histograms of observations nearest local noon. This same technique can be applied to B1 data, as demonstrated in Figure 3. The differences between the 80<sup>th</sup> percentile count and 5<sup>th</sup> percentile are plotted, showing a decrease of 1.8 counts per year (using linear regression). However, this analysis uses un-calibrated counts. A similar analysis will be used to explore the ISCCP calibration.

#### 4.2 Clouds

Cloud detection is generally the precursor to any satellite application which uses either the cloud pixels (e.g., precipitation analysis) or the clear-sky observations (e.g., albedo and aerosol retrievals). The ISCCP cloud detection algorithm (Rossow and Garder 1993a; Rossow and Garder 1993b) uses spatial and temporal tests to mask for clouds. The increased resolution provided by B1 data should provide a more accurate cloud detection algorithm (since the spatial tests will be

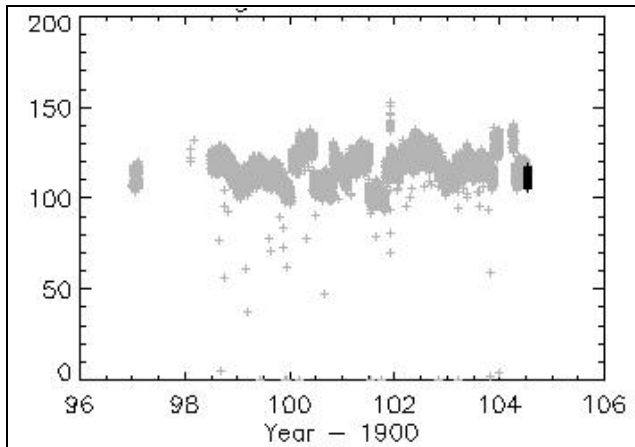


**Figure 2 – Time series of the average IR counts for the on-earth pixels for Meteosat-5.**

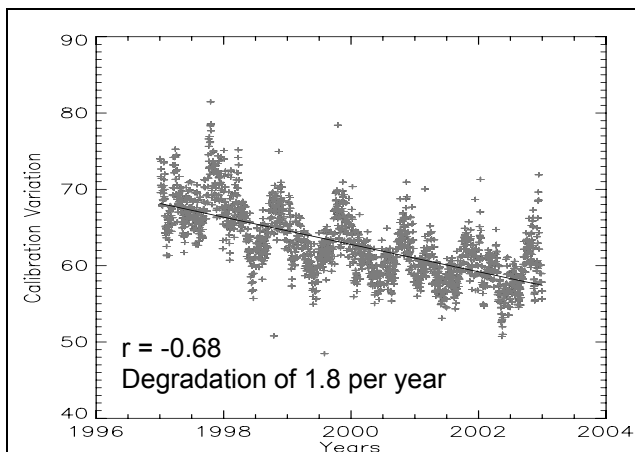


**Figure 3 – Meteosat-7 visible calibration analysis obtained through plotting the difference in image percentiles demonstrating a decrease in sensor response.**

better resolved). The increased resolution also will provide a cloud climatology at a higher spatial resolution than before, which will be beneficial to such industries as solar power.

#### 4.3 Aerosol

The B1 data set has the opportunity to provide the first visible observations of aerosol over land for the 20-year record. While polar-orbit observations exist, they are either limited to ocean observations (e.g., AVHRR, (Jacobowitz et al. 2003)) or inferred optical depths from ultraviolet wavelengths (e.g., TOMS, (Torres et al. 2002)). Techniques which allow aerosol optical depth retrievals from current sensors like the GOES Aerosol/Smoke Product (GASP), (Knapp et al.

2002) can be used to retrieve aerosol information for the B1 record.

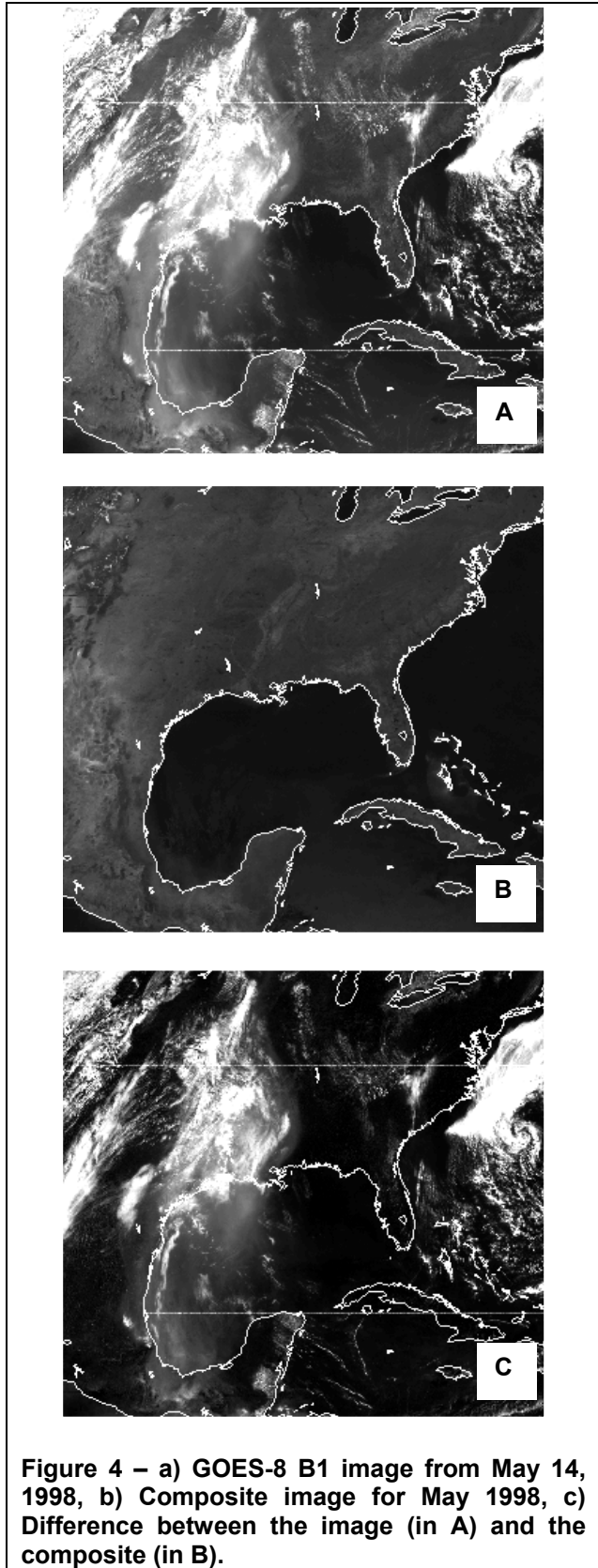
The example in Figure 4 demonstrates this concept. In general, a visible image (Fig. 4a) is composed of atmospheric and surface components. The surface component can be derived by compiling the darkest observation from a time series of observations from the same time of day (Fig 4b), and then the atmospheric component can be estimated using the difference (Fig. 4c). In this example, the atmospheric component shows clouds, but also vast amounts of aerosol transported to the U.S. during the Central American forest fires of May 1998. When this qualitative analysis is replaced by a quantitative one (using radiative transfer) the outcome is retrieved optical depth. From B1 data, this would be possible for most of the Earth's land masses (exceptions are deserts and snow covered land).

#### 4.4 Albedo

The albedo of the Earth's surface can be estimated from B1 imagery at a high (10 km) spatial resolution. The numerous observations from identical viewing geometry provide ample opportunity to observe a location free of clouds. A simplistic approach is to collect the darkest observation for each pixel over a given time-period. In the examples shown (Figure 5), the darkest pixels are collected for May 1998 for each satellite (nearest its local noon). Clearly, the variation in the Earth's reflectance can be observed. This, along with similar observations at different times of day (and, again, radiative transfer models with ancillary data) can provide an excellent estimate of the surface albedo.

#### 4.5 Surface Heating

Solar heating of the Earth's surface during forenoon hours (e.g., from 9:00 to 12:00 local time) primarily depends on the surface moisture and evapotranspiration (Tarpley 1988). As such, the heating rate is a primary candidate for assimilation into weather forecast models, since it provides valuable surface measurements where there are none. For example, an IR image from GOES-8 for May 18, 1998 at 17:45 is provided in figure 6a. The change in temperature (K) from 14:45 UTC is provided in figure 6b (no cloud mask has been applied, so clouds cause large changes in temperature, generally saturating the color scale at either black or white). In general, the changes over the ocean are less than  $\pm 1$  K, while over land, there is strong heating (in cloud-free regions). Also, some variation in the heating is apparent



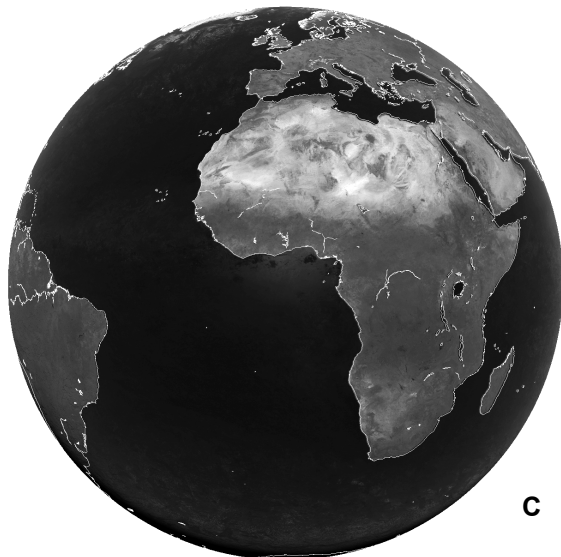
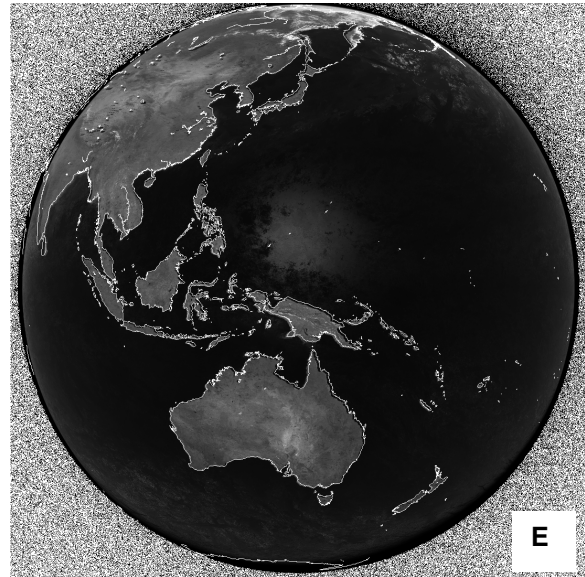
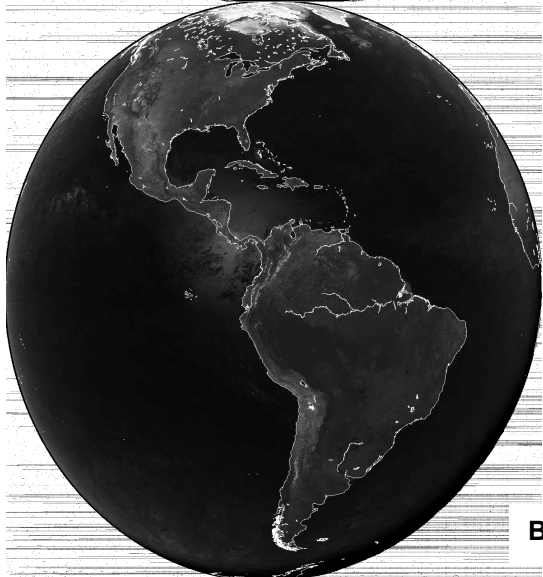
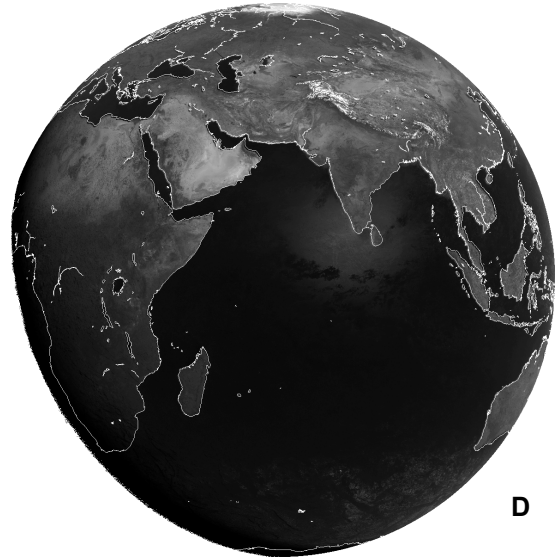
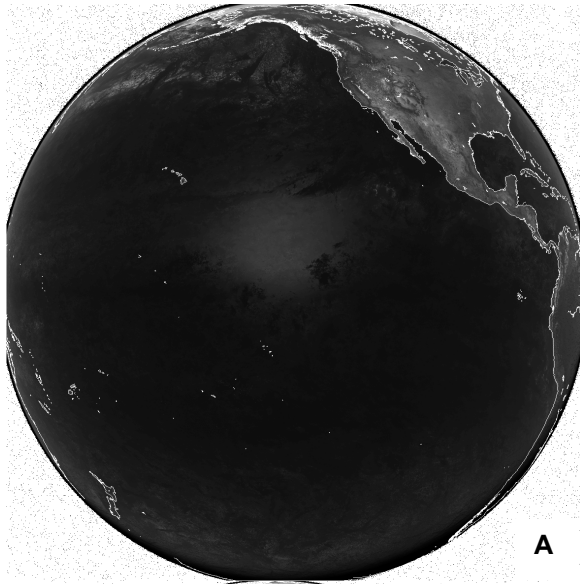
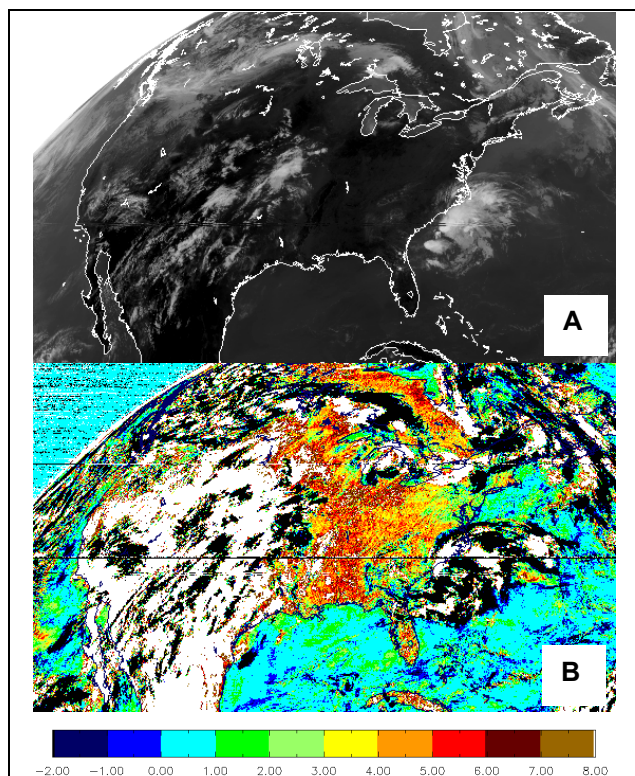


Figure 5 – Clear-sky composite imagery for May 1998 from a) GOES-10, b) GOES-8, c) Meteosat-7, d) Meteosat-5 and e) GMS-5.



**Figure 6 – a) Infrared image (11  $\mu\text{m}$ ) from GOES-8 B1 on 18 May 1998, 17:45 UTC b) 3-hour temperature change between part A and 14:45 UTC, demonstrating the ability to observe surface heating.**

over land. While this is a simple example, using more sophisticated assumptions (e.g., water vapor correction) and ancillary data can yield a climatology of heating rate for most of the world's land mass.

#### 4.6 Temporal/spatial variability

Global, 10 km data every three hours for

twenty years can provide a wealth of information on the climatic variations: from diurnal to inter-annual. For example, the diurnal trend in IR observations is shown in Figure 7 for June-July-August of 1999. The length of the arrow is proportional to the diurnal amplitude and the direction to the phase: maximum temperature at 00 UTC (up), 06 UTC (right), 12 UTC (down) and 18 UTC (left). Amplitudes are larger over land than ocean and in cloud free areas (deserts and western portions of continents). The time of maximum temperature follows the local time.

### 5. SUMMARY & FUTURE WORK

In summary, the B1 data set provides a unique view of the earth, rich with climate information covering the past twenty years. With the ongoing work to document the formats, and to test the quality and calibration, the B1 data can soon be used to develop long-term data sets for many atmospheric, land and ocean variables.

In spite of the extensive record, there are two significant data gaps. The GOES-East observation is missing for two time periods: 1992-1994 and 1996-1997. Specifically, GOES-7 data are missing from September 1992 through September 1994 (24 months) and GOES-8 data are missing from February 1996 through June 1997 (15 months). [These are the only data gaps of one month or longer]. In the future, these gaps will be filled in by sub-sampling the full resolution GOES data soon to be available through the Comprehensive Large Array-data Storage System (CLASS).

Another significant on-going effort is to convert the data to a uniform data format. Work is ongoing to determine the characteristics of the format (keeping as flexible as possible) to provide a format for past B1 data, but also for data from future satellites providing B1 data. The goal of the

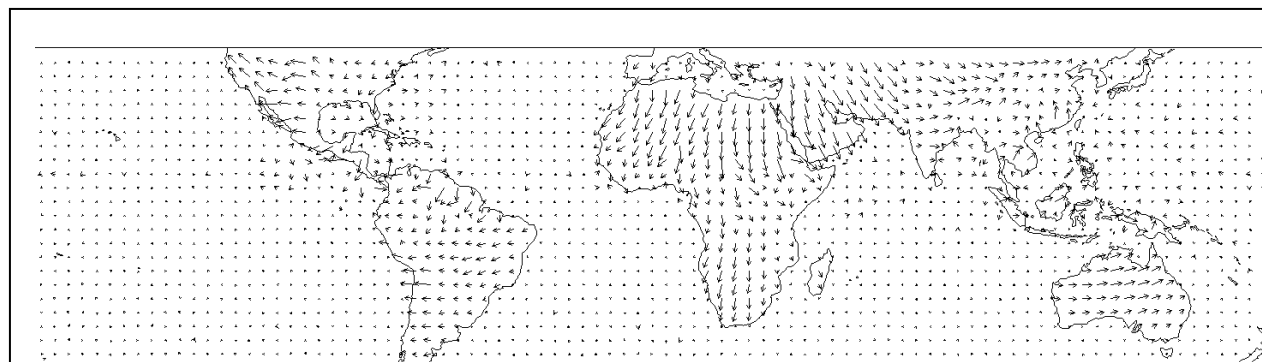


**Figure 7 - Diurnal trend in IR data for June-July-August 1999. Length of arrows is proportional to amplitude and the direction is proportional to time of maximum (up is 00UTC and right is 06UTC).**

effort is to limit the I/O formats to one type (currently, the B1 is in more than 10 separate data formats) and as few navigation algorithms as possible (currently, there are more than 5 navigation algorithms). Thus this research will be a significant benefit by providing a valuable resource for climate research.

## **ACKNOWLEDGMENTS**

Many scientists at all the SPCs and GPC were invaluable for their knowledge of ISCCP data.

## **REFERENCES**

- Jacobowitz, H., L. L. Stowe, G. Ohring, A. Heidinger, K. Knapp, and N. R. Nalli, 2003: The Advanced Very High Resolution Radiometer Pathfinder Atmosphere (PATMOS) Climate Dataset: A Resource for Climate Research. *Bulletin of the American Meteorological Society*, **84**, 785-793.
- Knapp, K. R., T. H. Vonder Haar, and Y. J. Kaufman, 2002: Aerosol optical depth retrieval from GOES-8: Uncertainty study and retrieval validation over South America. *Journal of Geophysical Research*, **107**, 10.1029/2001JD000505.
- Rigollier, C., M. Lefevre, P. Blanc, and L. Wald, 2002: The Operational Calibration of Images Taken in the Visible Channel of the Meteosat Series of Satellites. *Journal of Atmospheric and Oceanic Technology*, **19**, 1285-1293.
- Rossow, W. B. and L. C. Garder 1993a: Cloud Detection Using Satellite Measurements of Infrared and Visible Radiances for ISCCP. *Journal of Climate*, **6**, 2341-2369.
- Rossow, W. B. and L. C. Garder, 1993b: Validation of ISCCP Cloud Detections. *Journal of Climate*, **6**, 2370-2393.
- Tarpley, J. D., 1988: Some Climatological Aspects of Satellite-Observed Surface Heating in Kansas. *Journal of Applied Meteorology*, **27**, 20-29.
- Torres, O., P. K. Bhartia, J. R. Herman, A. Sinyuk, P. Ginoux, and B. N. Holben, 2002: A long-term record of aerosol optical depth from TOMS observations and comparison to AERONET measurements. *Journal of Atmospheric Science*, **59**, 398-413.